

# Precise quasielastic neutrino/nucleon cross section

Alessandro Strumia<sup>a</sup> and Francesco Vissani<sup>b</sup>

<sup>a</sup> *Dipartimento di Fisica dell'Università di Pisa e INFN, Italia*

<sup>b</sup> *INFN, Laboratori Nazionali del Gran Sasso, Theory Group, Italia*

## Abstract

Quasielastic antineutrino/proton and neutrino/neutron scatterings can be well approximated by simple formulæ, valid around MeV or GeV energies. We obtain a single expression valid in the whole range, and discuss its relevance for studies of supernova neutrinos, which reach intermediate energies.

## 1 Introduction

The quasielastic reaction  $\bar{\nu}_e p \rightarrow e^+ n$  (inverse beta decay) is of special relevance for studies of  $\bar{\nu}_e$  at sub-GeV energies [2]. Indeed, (1) its cross section is relatively large<sup>1</sup>,  $\sim G_F^2 E_\nu^2$ ; (2) it can be accurately computed; (3) it has a low threshold  $E_\nu > 1.806 \text{ MeV} \approx m_e + m_n - m_p$ ; (4) the measurable  $e^+$  energy is strongly correlated with the  $\bar{\nu}_e$  energy; (5) materials rich in free protons are cheap (e.g. water, hydrocarbon) and this permits to build large detectors; (6) in scintillators, it is possible to tag both the  $e^+$  and the neutron, reducing the backgrounds. These features are not shared by other reactions, e.g. (1), (4) and (6) do not hold for  $\nu e \rightarrow \nu e$  (since  $m_e \ll m_p$ );  $\bar{\nu}_e {}^{16}\text{O} \rightarrow e^+ {}^{16}\text{N}$  has high threshold  $E_\nu > 11.4 \text{ MeV}$  and it is theoretically much less clean.

The cross sections for quasielastic neutrino and antineutrino scattering on neutron or proton have been calculated long ago for applications at high energy  $E_\nu \sim \text{GeV}$  (e.g. accelerators). The reference formulæ for these applications are eqs. (3.18) and (3.22) in the review of Llewellyn-Smith [3], routinely used, for instance, in analyses of atmospheric neutrinos. Vogel and Beacom [4] remarked that effects suppressed by  $(m_n - m_p)/E_\nu$  have been neglected in eq. (3.22), which is a bad approximation at low energy  $E_\nu \sim \text{MeV}$  (e.g.  $\bar{\nu}_e$  generated by nuclear reactors or supernovæ). These authors proposed their eqs. (12) and (13) which, neglecting effects suppressed by powers of  $E_\nu/m_p$ , provide a simple and precise description of neutrino/nucleon scattering at low energy. In this paper, we derive a unique formula valid at low, intermediate and high energies, without assuming  $m_n - m_p \ll E_\nu$  nor  $E_\nu \ll m_p$ . We will compare our cross section with other approximations of common use, and discuss the range of energies where they are reliable. Our findings are relevant in particular for (1) detection of supernova  $\bar{\nu}_e$ , that can have an energy between few MeV up to about 60 MeV; (2) transport of  $e^\pm$ ,  $\nu_e$  and  $\bar{\nu}_e$  inside the collapsing star, where the effective temperatures are higher and neutrino energies can reach 200 MeV.

The cross-section is computed in section 2 and discussed in section 3.

<sup>1</sup>It is interesting to recall that the first authors who computed it [1] concluded: ‘*This meant that one obviously would never be able to see a neutrino.*’

## 2 Cross section

We write explicit expressions for inverse beta decay (IBD), namely quasielastic scattering of electron antineutrino on proton:

$$\bar{\nu}_e(p_\nu) + p(p_p) \rightarrow e^+(p_e) + n(p_n) \quad \text{IBD reaction.} \quad (1)$$

We indicate how to obtain the corresponding expressions for other antineutrinos  $\bar{\nu}_\mu$  and  $\bar{\nu}_\tau$ , and for quasielastic neutrino/neutron scattering. Let us define

$$\Delta = m_n - m_p \approx 1.293 \text{ MeV}, \quad M = (m_p + m_n)/2 \approx 938.9 \text{ MeV}. \quad (2)$$

The differential cross section at tree level in the weak interactions, averaged (summed) over initial (final) polarizations is:

$$\frac{d\sigma}{dt} = \frac{G_F^2 \cos^2 \theta_C}{2\pi(s - m_p^2)^2} |\mathcal{M}^2| \quad (3)$$

where  $G_F = 1.16637 \cdot 10^{-5} / \text{GeV}^2$  is the Fermi coupling extracted from  $\mu$ -decay,  $\cos \theta_C = 0.9746 \pm 0.0008$  [5] is the cosine of the Cabibbo angle and  $\mathcal{M}$  has the well-known current-current structure:

$$\mathcal{M} = \bar{\nu}_{\nu_e} \gamma^a (1 - \gamma_5) v_e \cdot \bar{u}_n \left( f_1 \gamma_a + g_1 \gamma_a \gamma_5 + i f_2 \sigma_{ab} \frac{q^b}{2M} + g_2 \frac{q_a}{M} \gamma_5 \right) u_p \quad (4)$$

where  $q = p_\nu - p_e = p_n - p_p$ . A straightforward calculation yields<sup>2</sup>:

$$|\mathcal{M}^2| = A(t) - (s - u)B(t) + (s - u)^2 C(t) \quad (5)$$

where  $s = (p_\nu + p_p)^2$ ,  $t = (p_\nu - p_e)^2$ ,  $u = (p_\nu - p_n)^2$  are the usual Mandelstam variables and

$$\begin{aligned} 16 A &= (t - m_e^2) \left[ 4|f_1^2|(4M^2 + t + m_e^2) + 4|g_1^2|(-4M^2 + t + m_e^2) + |f_2^2|(t^2/M^2 + 4t + 4m_e^2) + \right. \\ &\quad \left. + 4m_e^2 t |g_2^2|/M^2 + 8\text{Re}[f_1^* f_2](2t + m_e^2) + 16m_e^2 \text{Re}[g_1^* g_2] \right] \\ -\Delta^2 &\left[ (4|f_1^2| + t|f_2^2|/M^2)(4M^2 + t - m_e^2) + 4|g_1^2|(4M^2 - t + m_e^2) + 4m_e^2 |g_2^2|(t - m_e^2)/M^2 + \right. \\ &\quad \left. + 8\text{Re}[f_1^* f_2](2t - m_e^2) + 16m_e^2 \text{Re}[g_1^* g_2] \right] - 32m_e^2 M \Delta \text{Re}[g_1^*(f_1 + f_2)] \\ 16 B &= 16t \text{Re}[g_1^*(f_1 + f_2)] + 4m_e^2 \Delta (|f_2^2| + \text{Re}[f_1^* f_2 + 2g_1^* g_2]) / M \\ 16 C &= 4(|f_1^2| + |g_1^2|) - t|f_2^2|/M^2. \end{aligned} \quad (6)$$

In the limit  $\Delta = 0$  eq. (6) reduces to eq. (3.22) of Llewellyn-Smith.

Since strong interactions are invariant under  $T$  and  $C$ , the adimensional form factors  $f_i, g_i$  are real functions of the transferred 4-momentum  $t = q^2 < 0$ . As discussed in section 3.2 they can be approximated with [3]

$$\{f_1, f_2\} = \frac{\{1 - (1 + \xi)t/4M^2, \xi\}}{(1 - t/4M^2)(1 - t/M_V^2)^2}, \quad g_1 = \frac{g_1(0)}{(1 - t/M_A^2)^2}, \quad g_2 = \frac{2M^2 g_1}{m_\pi^2 - t} \quad (7)$$

<sup>2</sup>We give some details of the computation. The polynomial structure in  $s - u$  can be easily understood: if we express the leptonic tensor  $L^{ab}$  in terms of  $p_\ell = p_\nu + p_e$  and  $q$ , and the hadronic one  $H^{ab}$  in terms of  $p_h = p_p + p_n$  and  $q$ , it is sufficient to note that  $p_\ell \cdot p_h = s - u$  (while  $q^2 = t$ ,  $q \cdot p_\ell = -m_e^2$  and  $q \cdot p_h = m_n^2 - m_p^2 = 2M\Delta$ ). The dependence on  $\Delta$  of  $|\mathcal{M}^2|$  can be understood by deepening the same argument, namely: (1) one decomposes the leptonic tensor  $L^{ab}$  in 4 parts:  $p_\ell^a p_\ell^b$ ,  $q^a q^b - q^2 g^{ab}$ ,  $m_e^2 g^{ab}$ ,  $\epsilon^{abcd} p_{\ell c} q_d$ ; (2) then, one considers the general Lorentz-invariant decomposition of the hadronic tensor  $H(p_h, q)$  (6 parts); (3) finally, one checks explicitly the 24 contractions, and verifies that  $\Delta$  appears only in the combinations  $\Delta^2$  and  $m_e^2 \Delta$ .

where  $g_1(0) = -1.270 \pm 0.003$  [5],  $M_V^2 = 0.71 \text{ GeV}^2$ ,  $M_A^2 \approx 1 \text{ GeV}^2$ . Finally  $\xi = \kappa_p - \kappa_n = 3.706$  is the difference between the proton and neutron anomalous magnetic moments in units of the nuclear magneton ( $\kappa_p = 1.792$ ,  $\kappa_n = -1.913$ ).

The analogous expressions for  $\nu_e n$  scattering are obtained by exchanging  $p_\nu \leftrightarrow -p_e$ , and  $m_p \rightarrow m_n$  in the flux factor. Therefore,  $|\mathcal{M}^2|$  keeps the same expression with  $s - u \rightarrow u - s$ ; in view of its explicit form, this amounts to just replace  $B \rightarrow -B$  in eq. (5). The expressions for  $\nu_\mu$  or  $\nu_\tau$  scatterings are obtained by replacing  $m_e$  with  $m_\mu$  or  $m_\tau$ .

Our final expression is somewhat involved but allows to numerically compute any desired integrated cross-section. It is also useful to present some simple analytic approximation that is valid at low energies (say, at supernova and reactor energies or below). In fact, the  $\nu_e$ ,  $\bar{\nu}_e$  cross sections simplify, when expanding  $|\mathcal{M}^2|$  in powers of the parameter:

$$\varepsilon = E_\nu/m_p \quad (8)$$

When we prescribe that  $E_e, \Delta, m_e \sim \varepsilon$ , we get

$$s - m_p^2 \sim \varepsilon, \quad s - u \sim \varepsilon, \quad t \sim \varepsilon^2.$$

The flux factor in the denominator of  $d\sigma/dt$  gives a  $1/\varepsilon^2$ , and the amplitude  $|\mathcal{M}^2|$  starts at order  $\varepsilon^2$ . The leading order (LO) approximation in  $\varepsilon$  is obtained by retaining only

$$\begin{aligned} A &\simeq M^2(f_1^2 - g_1^2)(t - m_e^2) - M^2\Delta^2(f_1^2 + g_1^2) \\ B &\simeq 0 \\ C &\simeq (f_1^2 + g_1^2)/4 \end{aligned} \quad (9)$$

Since  $B \simeq 0$  at LO  $\nu_e n$  and  $\bar{\nu}_e p$  scatterings are described by the same  $\mathcal{M}^2$ .

A simple approximation which is accurate enough to describe the detection of supernova neutrinos events via IBD is obtained using the expression of  $\mathcal{M}^2$  accurate up to NLO in  $\varepsilon$ , given by

$$\begin{aligned} A &\simeq M^2(f_1^2 - g_1^2)(t - m_e^2) - M^2\Delta^2(f_1^2 + g_1^2) - 2m_e^2 M \Delta g_1(f_1 + f_2) \\ B &\simeq t g_1(f_1 + f_2) \\ C &\simeq (f_1^2 + g_1^2)/4 \end{aligned} \quad (10)$$

The  $t$  dependence of the form factors contributes at next order (NNLO): at NLO the form factors are approximated with constants.

## 2.1 Total cross section, $d\sigma/dE_e$ and event numbers

The cross section expressed in terms of the neutrino and electron energy in the rest frame of the proton,  $E_\nu$  and  $E_e$ , is particularly useful. Inserting

$$s - m_p^2 = 2m_p E_\nu, \quad s - u = 2m_p(E_\nu + E_e) - m_e^2, \quad t = m_n^2 - m_p^2 - 2m_p(E_\nu - E_e)$$

it is given by

$$\frac{d\sigma}{dE_e}(E_\nu, E_e) = 2m_p \frac{d\sigma}{dt} \quad \text{if } E_\nu \geq E_{\text{thr}} \equiv \frac{(m_n + m_e)^2 - m_p^2}{2m_p} \quad (11)$$

The allowed values of  $E_e$ ,  $E_1 \leq E_e \leq E_2$ , correspond to the possible scattering angles  $\theta^{\text{CM}}$  in the center of mass (CM) frame:

$$E_{1,2} = E_\nu - \delta - \frac{1}{m_p} E_\nu^{\text{CM}} (E_e^{\text{CM}} \pm p_e^{\text{CM}}), \quad \text{with } \delta \equiv \frac{m_n^2 - m_p^2 - m_e^2}{2m_p} \quad (12)$$

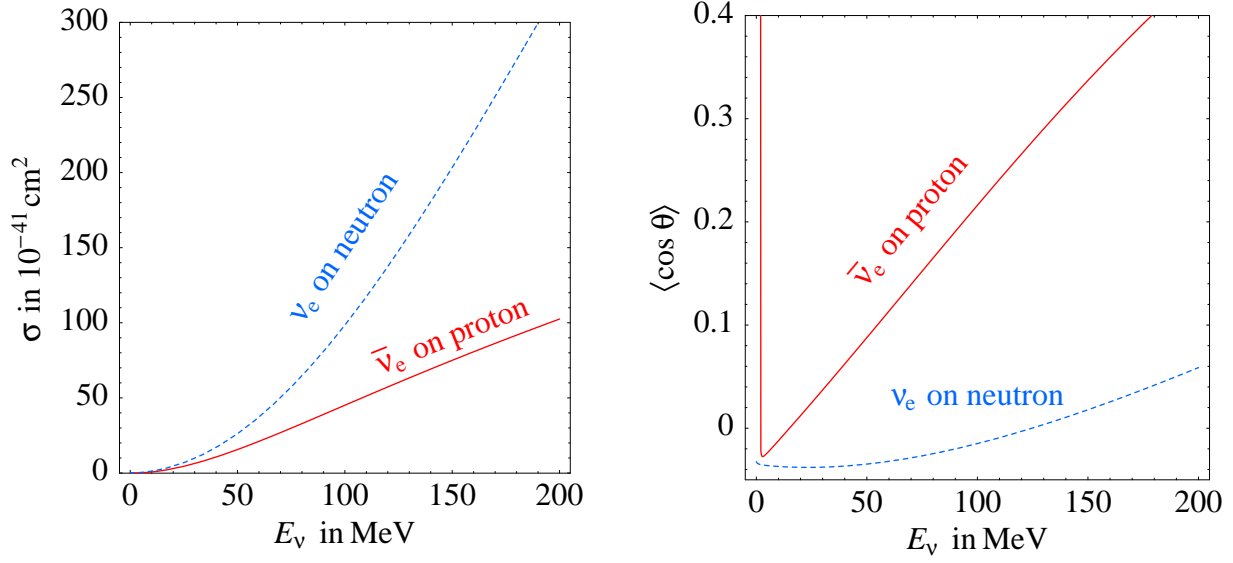


Figure 1: *Fig. 1a: total cross sections of quasielastic scatterings at supernova energies. Fig. 1b: average cosine of the charged lepton scattering angle  $\langle \cos \theta \rangle$ .*

where the energy and momenta in the CM have the standard expressions:

$$E_\nu^{\text{CM}} = \frac{s - m_p^2}{2\sqrt{s}}, \quad E_e^{\text{CM}} = \frac{s - m_n^2 + m_e^2}{2\sqrt{s}}, \quad p_e^{\text{CM}} = \frac{\sqrt{[s - (m_n - m_e)^2][s - (m_n + m_e)^2]}}{2\sqrt{s}} \quad (13)$$

For the neutrino reaction, one has just to replace  $m_n \leftrightarrow m_p$  in all formulæ above except in  $|\mathcal{M}^2|$ , where  $\Delta$  remains positive, with the proviso to set  $E_{\text{thr}} = 0$  for  $\nu_e$  (it would come negative). The total cross section is plotted in figure 1a and tabulated in table 1. We have included also two corrections:

1. the radiative corrections to the cross section [6, 7], well approximated as [7]

$$d\sigma(E_\nu, E_e) \rightarrow d\sigma(E_\nu, E_e) \left[ 1 + \frac{\alpha}{\pi} \left( 6.00 + \frac{3}{2} \log \frac{m_p}{2E_e} + 1.2 \left( \frac{m_e}{E_e} \right)^{1.5} \right) \right] \quad (14)$$

where  $\alpha$  is the fine-structure constant.

This one-loop correction is valid at  $E_\nu \ll m_p$ , when the final state positron (electron) is the only radiator, and in the hypothesis that all the energy  $E_e$  in electrons and bremsstrahlung photons is detected. In general the differential cross section is given by a more complicated expression which depends on detection threshold for photons. The total cross section is still given by eq. (14), if all final state electrons are detected [7].

High-energy electroweak corrections are automatically included in the values of  $g_1(0)$  and  $G_F$  extracted from low-energy experiments.

2. We multiply  $\sigma(\nu_e n \rightarrow pe)$  by the Sommerfeld factor that accounts for final-state interactions:

$$F(E_e) = \frac{\eta}{1 - \exp(-\eta)}, \quad \text{with } \eta = \frac{2\pi\alpha}{\sqrt{1 - m_e^2/E_e^2}} \quad (15)$$

$E_\nu$	$\sigma(\bar{\nu}_e p)$	$\langle E_e \rangle$	$\langle \cos \theta \rangle$	$E_\nu$	$\sigma(\bar{\nu}_e p)$	$\langle E_e \rangle$	$\langle \cos \theta \rangle$	$E_\nu$	$\sigma(\bar{\nu}_e p)$	$\langle E_e \rangle$	$\langle \cos \theta \rangle$
1.806	0	—	—	8.83	0.511	7.46	-0.015	43.2	12.1	40.2	0.070
2.01	0.00351	0.719	-0.021	9.85	0.654	8.47	-0.013	48.2	14.7	44.8	0.083
2.25	0.00735	0.952	-0.025	11.0	0.832	9.58	-0.010	53.7	17.6	49.9	0.097
2.51	0.0127	1.21	-0.027	12.3	1.05	10.8	-0.007	59.9	21.0	55.6	0.113
2.80	0.0202	1.50	-0.027	13.7	1.33	12.2	-0.003	66.9	25.0	61.8	0.131
3.12	0.0304	1.82	-0.027	15.3	1.67	13.7	0.0006	74.6	29.6	68.8	0.151
3.48	0.0440	2.18	-0.027	17.0	2.09	15.5	0.005	83.2	34.8	76.5	0.173
3.89	0.0619	2.58	-0.026	19.0	2.61	17.4	0.010	92.9	40.7	85.0	0.198
4.33	0.0854	3.03	-0.025	21.2	3.24	19.5	0.015	104.	47.3	94.5	0.225
4.84	0.116	3.52	-0.024	23.6	4.01	21.8	0.021	116.	54.6	105.	0.255
5.40	0.155	4.08	-0.023	26.4	4.95	24.4	0.028	129.	62.7	117.	0.288
6.02	0.205	4.69	-0.022	29.4	6.08	27.3	0.036	144.	71.5	130.	0.323
6.72	0.269	5.38	-0.020	32.8	7.44	30.5	0.044	160.	81.0	144.	0.361
7.49	0.349	6.15	-0.018	36.6	9.08	34.1	0.054	179.	91.3	161.	0.400
8.36	0.451	7.00	-0.016	40.9	11.0	38.0	0.065	200.	102.	179.	0.442

Table 1: Values of  $\sigma(\bar{\nu}_e p \rightarrow ne^+)$  in  $10^{-41} \text{ cm}^2$  and of the average positron energy and cosine of the scattering angle. All energies are in MeV.

Both the radiative corrections and final state interactions amount to a  $\sim 2\%$  correction, which can be important for high statistic data samples.

The formulæ given above can be adapted to the case when the nucleon is not at rest (e.g. inside a supernova). Similarly, one can include Fermi blocking-factors in final state to account for degenerate electrons sea in the supernova.

It is straightforward to compute the average values  $\langle x \rangle = \int x d\sigma / \int d\sigma$  of interesting kinematical quantities  $x$ , like  $x = E_e$ ,  $E_e^2 - \langle E_e \rangle^2$ ,  $\cos \theta$ , etc. We plot in figure 2 and tabulate in table 1 the average cosine of the scattering angle of the charged lepton. Detecting supernova neutrinos via the IBD reaction, one could try to track their source by measuring the direction of positrons, that are copiously produced [8, 4] (more discussion below). Another important quantity is the average lepton energy, which can be approximated (at better than 1% below  $\sim 100$  MeV) by

$$\langle E_e \rangle \approx (E_1 + E_2)/2 = E_\nu - \delta - E_\nu^{\text{CM}} E_e^{\text{CM}} / m_p \quad (16)$$

This is a much better approximation than the usual formula  $E_e = E_\nu - \Delta$ ; it permits to relate  $E_e$  with  $E_\nu$  incorporating a large part of the effect due to the recoil of the nucleon.

It is straightforward to include cuts or efficiencies: e.g., if the positrons are detected only in the window  $E_l \leq E_e \leq E_h$  we define

$$\sigma(E_\nu) = \int_{E_1}^{E_2} dE_e \frac{d\sigma}{dE_e}(E_\nu, E_e) \vartheta(E_e - E_l) \vartheta(E_h - E_e) \quad (17)$$

where  $\vartheta(x)$  is the step function, equal to 0 (1) for  $x < 0$  ( $x > 0$ ). The total number of events in the detector and the distribution in positron energy are given by

$$N_{e^+} = N_p \int dE_\nu \frac{d\Phi}{dE_\nu} \sigma(E_\nu) \quad \frac{dN_{e^+}}{dE_e} = N_p \int dE_\nu \frac{d\Phi}{dE_\nu} \frac{d\sigma}{dE_e} \quad (18)$$

where  $N_p$  is the number of target protons and  $\Phi$  is the  $\bar{\nu}_e$  flux. We do not have a simple formula for the exact limits of integration in  $dE_\nu$ . A simple recipe is to integrate numerically in the larger range

$$E_e + \delta \leq E_\nu \leq \frac{E_e + \delta}{1 - 2(E_e + \delta)/m_p} \quad (19)$$

obtained replacing  $p_e^{\text{CM}}$  and  $E_e^{\text{CM}}$  with  $E_\nu^{\text{CM}}$  in eq. (12), enforcing the correct kinematical range by means of  $\vartheta$ -functions; the upper limit has to be replaced with infinity when the denominator becomes negative.

## 2.2 Angular distribution

The cross section differential in the angle  $\theta$  between the neutrino and the positron is obtained from  $d\sigma/dt$  after including the Jacobian coming from  $t = m_e^2 - 2E_\nu(E_e - p_e \cos \theta)$ :

$$\frac{d\sigma}{d \cos \theta}(E_\nu, \cos \theta) = \frac{p_e \varepsilon}{1 + \varepsilon(1 - \frac{E_e}{p_e} \cos \theta)} \frac{d\sigma}{dE_e}, \quad (20)$$

where  $\varepsilon = E_\nu/m_p$ . In eq. (20),  $E_e$  and  $p_e$  are functions of  $E_\nu$  and  $\theta$ :

$$E_e = \frac{(E_\nu - \delta)(1 + \varepsilon) + \varepsilon \cos \theta \sqrt{(E_\nu - \delta)^2 - m_e^2 \kappa}}{\kappa}, \quad p_e = \sqrt{E_e^2 - m_e^2} \quad (21)$$

with  $\kappa = (1 + \varepsilon)^2 - (\varepsilon \cos \theta)^2$ . A lepton of low energy cannot be emitted in all directions  $\theta = 0 \div \pi$ , since it is “dragged” by the motion of the CM.<sup>3</sup> The  $\tau$ , being heavier than the proton, is always emitted in the forward cone. For  $\bar{\nu}_e$  or  $\bar{\nu}_\mu$  a non trivial allowed range of  $\theta$  is obtained only in a very small region energy range just above the threshold  $E_{\text{thr}}$  (given in eq. (11)):

$$E_{\text{thr}} \leq E_\nu \leq E'_{\text{thr}} = E_{\text{thr}} + m_e \frac{[m_n - (m_p - m_e)]^2}{2m_p(m_p - m_e)} \quad (22)$$

For the muon (electron),  $E'_{\text{thr}} - E_{\text{thr}} = 0.8 \text{ MeV}$  (1 eV). Above  $E'_{\text{thr}}$  all scattering angles are allowed. Therefore, we can conveniently simplify  $\bar{\nu}_e$ ,  $\bar{\nu}_\mu$ , scatterings by replacing  $E_{\text{thr}}$  with  $E'_{\text{thr}}$  and considering the full range  $\theta = 0 \div \pi$ . This is a very good approximation.

## 3 Discussion and applications

How important is to use an accurate cross section, or in other words, what is the error that we introduce when we use an approximate cross section, instead of the correct one? The answer, of course, depends on the process we are considering. Here we compare our cross section with other ones that can be found in the literature, evaluate its uncertainty, and finally discuss the specific application for supernova  $\bar{\nu}_e$  signal.

Here we mention some other possible applications of these results. A precise cross section can be used in an accurate description of neutrino transport in a collapsing supernova (see e.g. [9] for some

<sup>3</sup>The region of “CM-dragging” is defined by the condition that the CM velocity  $\beta$  is larger than  $\beta_e^{\text{CM}}$ . In this region, the function  $\theta^{\text{CM}}(\theta)$  — or  $\theta^{\text{CM}}(t)$  or  $\theta^{\text{CM}}(E_e)$  — is not single-valued: there are two values of  $\theta^{\text{CM}}$  that lead to the same  $\theta$ . This is evident from the relation  $\tan \theta = \sin \theta^{\text{CM}} / [\gamma(\cos \theta^{\text{CM}} + \beta/\beta_e^{\text{CM}})]$  where  $\gamma = 1/\sqrt{1 - \beta^2}$ . The region of ‘dragging’ is visible in the leftmost part of figure 2: it is where the curve “ $\bar{\nu}_e$  on proton” rises suddenly. Exactly at the threshold, the positron is emitted only at  $\theta = 0$ , so that  $\langle \cos \theta \rangle \rightarrow 1$ .

$E_\nu$ , MeV			2.5	5	10	20	40	80	160
Percentage difference in $\sigma(\bar{\nu}_e p \rightarrow n\bar{e})$									
1	Naïve	***	-3.9	-5.8	-9.9	-19	-38	-84	-210
2	Naïve +	***	0	0.3	-0.2	0.4	0.2	0.5	-0.9
3	Vogel and Beacom	**	0	0	0.3	1.2	5.6	28	150
4	NLO in $E_\nu/m_p$	*	0	0	0	0	0.1	1.5	13
5	Horowitz	**	-370	-83	-32	-14	-6.4	-3.0	-1.3
6	Llewellyn-Smith +	*	-13	-2.1	-0.5	-0.1	0	0	0
7	LS + VB	*	0.5	0.1	0	0	0	0	0
Percentage difference in $\sigma(\nu_e n \rightarrow pe)$									
1	Naïve	***	-1.7	-1.5	-1.0	-0.4	0.2	-1.5	-14
4	NLO in $E_\nu/m_p$	***	0	0	0	-0.1	-0.5	-2.4	-12
5	Horowitz	**	56	37	22	12	6.3	3.2	1.6
6	Llewellyn-Smith +	*	-3.9	-1.2	-0.3	-0.1	0	0	0

Table 2: *Percentage difference between our full result and various approximations for  $\bar{\nu}_e$  (above) and  $\nu_e$  (below) total cross sections. A negative (positive) sign means that a certain cross section is an over(under)-estimate. It is easy to implement approximations made with \*\*\*, while implementing those marked with a \* is not much simpler than performing a full computation.*

recent calculations). We recall that neutrino heating (or more generally, the coupling of neutrinos with the deepest layers of the mantle) takes place at energies  $E_\nu$  of several tenths of MeV, and it is regulated by the cross sections that we are discussing. Furthermore, electron neutrinos with energies in the range 50 – 150 MeV are particularly important for the dynamics of neutrino emission: they are around the Fermi surface of the degenerate neutrino distribution, and determine the neutrino flux from the inner core.

A precise cross section should also be used to interpret searches for  $\bar{\nu}_e$  or  $\bar{\nu}_\mu$  low energy neutrinos from the sun (see e.g. [10]), from gamma-ray-burst or other presently unknown cosmic sources [11]; or also, in studies of  $\nu_\mu$  or  $\bar{\nu}_\mu$  interactions just above the threshold of  $\mu$  production (e.g., for large sample of data in terrestrial experiments).

The LSND and KARMEN experiments [12] used a  $\bar{\nu}_\mu$  flux with a continuous spectrum up to 52.8 MeV, mainly produced by  $\mu^+$  decay at rest, looking for  $\bar{\nu}_e$  appearance using the  $\bar{\nu}_e p \rightarrow e^+ n$  reaction. The experimental result is controversial. If such a signal exists, a precise computation of the  $\bar{\nu}_e p$  cross-section would be necessary to interpret a more precise future experiment.

### 3.1 Comparison with various simple approximations

Table 2 shows the percentage difference

$$\delta\sigma = 100 \times (1 - \sigma'/\sigma) \quad (23)$$

between our cross section  $\sigma$  and various approximations  $\sigma'$ , evaluated at the same input parameters (percentages below 0.1% have been set to zero). The first row shows the neutrino energies at which the comparison is made. In the upper panel we consider the  $\bar{\nu}_e$  reaction; in the lower panel the  $\nu_e$  reaction.

1. The **naïve** low-energy approximation (see e.g. [13])

$$\sigma \approx 9.52 \times 10^{-44} \frac{p_e E_e}{\text{MeV}^2} \text{ cm}^2, \quad E_e = E_\nu \pm \Delta \text{ for } \bar{\nu}_e \text{ and } \nu_e, \quad (24)$$

obtained by normalizing the leading-order result to the neutron lifetime, overestimates  $\sigma(\bar{\nu}_e p)$  especially at high energy. It is not recommended for analyses of supernova neutrinos, nor for precise studies of reactor  $\bar{\nu}_e$ . The naïve  $\sigma(\nu_e n)$ , instead, agrees well with the exact cross section.

2. A simple approximation which agrees with our full result within few per-mille for  $E_\nu \lesssim 300$  MeV is

$$\sigma(\bar{\nu}_e p) \approx 10^{-43} \text{ cm}^2 p_e E_e E_\nu^{-0.07056+0.02018 \ln E_\nu - 0.001953 \ln^3 E_\nu}, \quad E_e = E_\nu - \Delta \quad (25)$$

where all energies are expressed in MeV.

3. The low-energy approximation of **Vogel and Beacom** [4] (which include first order corrections in  $\varepsilon = E_\nu/m_p$ , given only for antineutrinos) is very accurate at low energies ( $E_\nu \lesssim 60$  MeV), however underestimates the number of supernova IBD neutrino events at highest energies by 10%. Higher order terms in  $\varepsilon$  happen to be dominant already at  $E_\nu \gtrsim 135$  MeV, where the expansion breaks down giving a negative cross-section [4, 14].
4. The **NLO** low-energy approximation, defined by eq. (10), can be used from low energies up to the energies relevant for supernova  $\bar{\nu}_e$  detection. (We expand the squared amplitude in  $\varepsilon$  but, unlike Vogel and Beacom we treat kinematics exactly, so that some higher order terms are included in our NLO cross section).
5. The high-energy approximation of **Horowitz** [14], obtained from the Llewellyn-Smith formulæ setting  $m_e = 0$ , was not tailored to be used below  $\sim 10$  MeV, and it is not precise in the region relevant for supernova neutrino detection; however, it is presumably adequate to describe supernova neutrino transport.
6. The **Llewellyn-Smith** high-energy approximation, improved adding  $m_n \neq m_p$  in  $s, t, u$ , but not in  $\mathcal{M}$  is very accurate at all energies relevant for supernova neutrinos, failing only at the lowest energies. As proved in section 2, this is a consequence of the absence in  $|\mathcal{M}^2|$  of corrections of order  $\Delta/m_p$ .
7. Finally, approximation 6. can be improved by including also the dominant low-energy effects in the amplitude  $\mathcal{M}$ , as discussed in section IIB of [4]. With respect to our full result, this amounts to neglect  $\Delta$  and  $m_e$  in  $A, B, C$ , eq. (6), and reinsert part of them modifying  $A \rightarrow A - 4M^2\Delta^2C$ . This approximation agrees with our full result within few per mille.

### 3.2 Overall uncertainty

We now discuss how accurate our full expressions for the cross sections are. All input quantities have been precisely measured, except the  $t$ -dependence of the form factors of eq. (7). As shown in section 2, it affects the cross sections only at NNLO in  $E_\nu/m_p$ . In practice, taking the form factors as constants overestimates the total  $\bar{\nu}_e p$  and  $\nu_e n$  cross sections by about  $1\% \cdot (E_\nu/40 \text{ MeV})^2$ . At low energy this is an excellent approximation, and the dominant uncertainty is due to  $\theta_C$  and  $g_1(0)$ . The values we adopted are extracted from different sources. The Cabibbo angle  $\theta_C$  is extracted independently from  $V_{us}$  (measured from  $K_{\ell 3}$  decays) and from  $V_{ud}$  (measured from nuclear decays dominated by vectorial matrix elements, and from neutron decay). Since the two determinations agree only within  $2.2\sigma$  and theoretical errors play an important rôle, the total error has been conservatively increased [5].

The axial coupling  $g_1(0)$  is measured from neutron decay<sup>4</sup>. Different experimental determinations do not fully agree, therefore we conservatively increased the error. Newer measurements, performed

---

<sup>4</sup>Its uncertainty is fully correlated with the uncertainty on the  $\theta_C$  determination from neutron decay, since neutron decay measures the same combination of  $g_1(0)$  and  $\theta_C$  that enters in IBD.



with a higher neutron polarization than older ones, are consistent and agree on  $g_1(0)/f_1(0) = -1.272 \pm 0.002$  when older determinations are discarded — a value slightly different from the one quoted in section 2. Isospin-breaking corrections to  $f_1(0) = 1$  are negligible [15].

In conclusion, at low energy  $\sigma(\bar{\nu}_e p)$  has an overall 0.4% uncertainty, which is adequate for present experiments. The ratio between the measured and the no-oscillation reactor  $\bar{\nu}_e$  flux is  $1.01 \pm 2.8\%(\text{stat}) \pm 2.7\%(\text{syst})$  at CHOOZ [16]. The KamLAND collaboration presently has a 6% systematic error on their reactor  $\bar{\nu}_e$  data [17], and aims at reaching the 4% level in future. Concerning supernova  $\bar{\nu}_e$ , experiments should collect few hundreds to several thousand of events, depending on when and where the next galactic supernova explosion will occur [2, 18, 19].

We finally discuss the uncertainty introduced by the  $t$  dependence of the form factors, which for the largest supernova  $\bar{\nu}_e$  or  $\nu_e$  energies is not fully negligible. The SU(2) isospin symmetry (broken only by small quark masses and by electromagnetism) allows to relate the vector form factors  $f_1$  and  $f_2$  to measured  $eN$  cross sections, and conservation of the vector current predicts  $f_1(0) = 1$ . The first terms in the expansion in  $t$

$$f_1(t) \simeq 1 + 2.5t/\text{GeV}^2, \quad f_2(t) \simeq \xi[1 + 3.4t/\text{GeV}^2]$$

are known with about 1% accuracy [20]. The phenomenological parametrization in eq. (7), partially suggested by theoretical considerations, reproduces reasonably well the experimental data. Employing slightly more accurate parametrizations for the vector form factors  $f_1$  and  $f_2$  (e.g. [20]) would not improve the accuracy of our results due to the larger uncertainty on the axial form factors  $g_1$  and  $g_2$ .

The axial form factor  $g_2$  (written in eq. (7) in terms of  $g_1$ , as suggested partial conservation of the axial current) has a negligible impact on  $\nu_e$  and  $\bar{\nu}_e$  scattering at intermediate energies. Thus, the main uncertainty comes from  $g_1$ . Vector meson dominance would suggest  $g_1 = g_1(0)/(1 - t/M_{A_1}^2)$  where  $M_{A_1} = (1.23 \pm 0.04)$  GeV is the mass of the pseudo-vector that, mixing with the  $W$  boson, should give the dominant effect. The parametrization of  $g_1$  adopted in eq. (7) is obtained by squaring  $(1 - t/M_A^2)$  and leaving  $M_A$  as a free parameter because this provides a better fit of data. Lattice simulations do not contradict this hypothesis within the present theoretical errors, that are however still large [21]. Assuming that the parametrization is correct, one obtains

1.  $M_A = (1.069 \pm 0.016)$  GeV [22] from  $\pi$  electroproduction on nucleons ( $\gamma^* N \rightarrow \pi N'$ ). The presence of  $\pi$  makes this probe experimentally precise but theoretically uncertain, as we are interested in  $\langle n | \dots | p \rangle$ , not in  $\langle \pi n | \dots | p \rangle$ .
2.  $M_A = (1.026 \pm 0.021)$  GeV [23, 22] from global fits of  $\nu N$  scattering data. Most of the data are not taken at  $|t| \ll \text{GeV}^2$ , where the parametrization of  $g_1$  is certainly justified.
3.  $\mu$  capture on  $p$  could provide a clean and direct probe of  $g_2$  at  $t = -0.88m_\mu^2$ . The present experimental data [24] hint to a value about 50% larger than the one we assume<sup>5</sup>, but their interpretation is under debate [22]. New data should clarify the issue [25].

The above discussion shows why it is difficult to assess the uncertainty on  $g_1$  and  $g_2$ . Optimistically assuming that 1. or 2. is right, it is negligible. On the other side, a pessimistic estimate can be obtained by using  $M_{A_1}$  in place of  $M_A$ : the total  $\bar{\nu}_e p$  cross section increases by  $0.4\%(E_\nu/50 \text{ MeV})^2$  for  $E_\nu \lesssim 200 \text{ MeV}$ . The shift remains relatively small because, as shown in section 2, the  $t$ -dependence of the form factors affects  $\bar{\nu}_e p$  only at NNLO in  $E_\nu/m_p$ .

---

<sup>5</sup>Such an increase of  $g_2$  has some impact on  $\nu_\mu$  and  $\bar{\nu}_\mu$  scattering, and would decrease  $\sigma(\bar{\nu}_\mu p)$  by  $3.8\% \times (150 \text{ MeV}/E_\nu)^3$ .

### 3.3 Search for relic supernova neutrinos

Here we discuss the application of our cross section to the search for neutrino radiation from past core-collapse supernovæ. We focus on the energy range  $E_e > 20$  MeV which is particularly suited for this type of search, since it contains a large part of the expected signal and it is largely free from background (for an experimental proof, see [26]). We assume that the energy distribution of supernova  $\bar{\nu}_e$  in the detectors is described by the following differential flux (see e.g. [9, 18]):

$$\frac{d\Phi}{dE_\nu} = \frac{E_{\text{tot}}}{4\pi D^2} \left[ \frac{f_e}{T_e^2} \cos^2 \theta_{12} n\left(\frac{E_\nu}{T_e}\right) + \frac{f_{\mu,\tau}}{T_{\mu,\tau}^2} \sin^2 \theta_{12} n\left(\frac{E_\nu}{T_{\mu,\tau}}\right) \right] \quad (26)$$

where 1)  $\theta_{12} \approx 34^\circ$  describes ‘solar’ oscillations in supernova mantle; 2)  $n(x) = 120x^2/7\pi^4[1 + e^x]$  is the Fermi-Dirac occupation factor; 3)  $f_e \approx 1/5$  and  $f_{\mu,\tau} \approx 1/7$  are the energy shares in  $\bar{\nu}_e$  and in  $\bar{\nu}_{\mu,\tau}$ ; 4)  $T_e \sim \text{few MeV}$  is the temperature of  $\bar{\nu}_e$  (before oscillations) and 5)  $T_{\mu,\tau}$  is the temperature of  $\bar{\nu}_{\mu,\tau}$ , that we assume to be  $T_{\mu,\tau} \approx 1.3 \times T_e$ ; 6)  $E_{\text{tot}}$  is the total energy released in neutrinos,  $D$  the distance of the supernova. We neglect various effects that would not change our conclusions, like ‘pinching’ of the spectrum (i.e. non-thermal effects), eventual oscillations in the Earth, existence of other detection reactions (we focus on detectors with a large fraction of free protons like water Čerenkov or scintillators), precise definition of the search window (which depends on the background level), detector efficiencies, other oscillations eventually induced by a non-vanishing  $\theta_{13}$ , etc.

We compare the expected number of events  $N_{e^+}$  in the energy range  $E_e = [20, 40]$  MeV using (a) the cross section of eq. (17) and (b) the naïve (and much used) cross section in eq. (24). The latter leads to an overestimate:

$$100 \times \left( 1 - \frac{N_{e^+}(\text{b})}{N_{e^+}(\text{a})} \right) \approx -25\% + 2.4\% \times x, \quad \text{where} \quad x = \frac{T_e - 4.5 \text{ MeV}}{\text{MeV}}. \quad (27)$$

The Super-Kamiokande collaboration presently gives the dominant bound on the relic  $\bar{\nu}_e$  flux, constrained to be less than  $1.2\bar{\nu}_e/\text{cm}^2\text{s}$  at 90% CL for  $E_\nu > 19.3$  MeV [26] — slightly above the flux expected by cosmological models [27]. Since this bound has been obtained assuming the naïve  $\bar{\nu}_e p$  cross section, eq. (27) suggests that it could be weakened by  $\sim 20\%$  (a reanalysis of the data with a precise cross section would allow to be more precise). Similar considerations apply to certain calculations of the expected event number from next galactic supernova (e.g. ref. [19]) and to estimates of the total energy  $E_{\text{tot}}$  from SN1987A neutrino data (e.g. ref. [28]), although the low energy cuts are typically smaller than 20 MeV and therefore the inaccuracy is less severe.

### 3.4 Low energy atmospheric neutrinos as a background

Low energy atmospheric neutrinos constitute a background for searches of relic supernova neutrinos. At Super-Kamiokande [26], this background is mostly due to muons produced below the Čerenkov threshold in water ( $E_\mu < 160$  MeV), whose decay produces a positron. Assuming that at low energy the  $\bar{\nu}_\mu$  flux scales as  $\sim 1/E_\nu$  [29], the cross section with  $m_p = m_n = M$  overestimates the background only by 1.5%. This is smaller than what suggested by a simple minded estimate, performed looking at the total cross section without taking into account that the condition that the muon is produced below the Čerenkov threshold *does depend* on  $\Delta = m_n - m_p$ . Similar considerations apply to the  $\bar{\nu}_e$  atmospheric neutrino background: e.g., the use of the Llewellyn-Smith cross section for  $E_e = [50, 80]$  MeV introduces a 2.4% overestimate.

### 3.5 Distributions of positrons from supernova neutrinos

Now we compute the energy and scattering-angle distribution of positrons generated by supernova  $\bar{\nu}_e$  and detected via the IBD cross section, that we compute according to the formulæ of sections 2.1 and

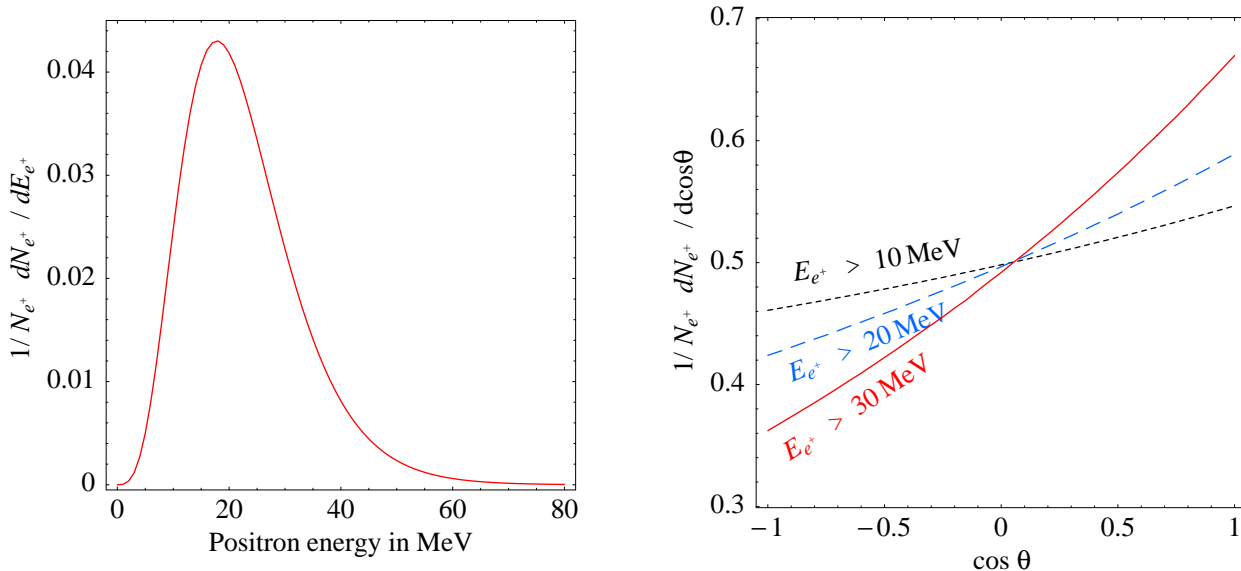


Figure 2: Fig. 2a shows the energy spectrum of positrons. Fig. 2b shows the positron scattering angle distribution, for different lower cuts on the positron energy. We assume that supernova  $\bar{\nu}_e$  have the flux in eq. (26) and are detected via the  $\bar{\nu}_e p \rightarrow n e^+$  reaction.

2.2. Again, we assume the  $\bar{\nu}_e$  flux of eq. (26), where we set  $T_e = 4.5$  MeV. The result is shown in fig. 2. The average cosine of the scattering angle asymmetry is approximatively given by

$$\langle \cos \theta \rangle = 0.024 + 0.013 x \quad (28)$$

( $x$  as in eq. (27)) which means that the scattering is slightly forward. The forward/backward asymmetry is not particularly large, but could be observed in a large sample of neutrinos from a galactic core-collapse supernova using wisely designed selection criteria (such as an energy dependent angular analysis). For example, it is sufficient to increase the lower cut on the positron energy to increase the asymmetry considerably

$$\langle \cos \theta \rangle = \begin{cases} 0.028 & \text{for } E_e > 10 \text{ MeV} \\ 0.055 & \text{for } E_e > 20 \text{ MeV} \\ 0.102 & \text{for } E_e > 30 \text{ MeV} \end{cases} \quad (T_e = 4.5 \text{ MeV}). \quad (29)$$

as more precisely illustrated in fig. 2b. A lower cut on  $E_e$  increases  $\langle \cos \theta \rangle$  for two different reasons: because the IBD reaction is forward peaked at higher energy, and because forward positrons are more energetic. (In the Super-Kamiokande detector a lower cut  $E_e \gtrsim 8$  MeV must anyhow be imposed in order to cut low energy backgrounds). Two remarks are in order: 1) An accurate description of the direction of IBD events is also important to separate other classes of events, as those due to reactions with Oxygen nuclei in water Čerenkov detectors. 2) An accurate description of the spectrum is particularly important when trying to extract information from the high energy tail of the distribution, about e.g. oscillations in the Earth, or non-thermal corrections to the energy spectrum.

Of course, not only  $\langle \cos \theta \rangle$  but also the number of events  $N_{e^+}$  depends on the temperature. Assuming unit efficiency above  $E_e = 8$  MeV and using eq. (18), we find that varying  $T_e$  around the reference temperature, the number of events varies approximately as  $1 + 0.24x - 0.02x^2$ :  $N_{e^+}$  increases (decreases) by 23% (26%) for  $T_e = (4.5 \pm 1)$  MeV.

## Acknowledgments

We thank G. Battistoni, V. Berezinsky, S. Capitani, A. Ianni, G. Isidori, H.T. Janka, A. Kurylov, M. Malek, D. Nicolò, E. Oset, O. Palamara and K. Sato for clarifying discussions and J.F. Beacom and W. Fulgione for the initial encouragement.

## References

- [1] H.A. Bethe and R. Peierls, *Nature* 133,(1934) 532.
- [2] For a recent review see e.g. F. Ci, *Int. J. Mod. Phys. A17* (2002) 1765 (hep-ex/0202043).
- [3] C.H. Llewellyn-Smith, *Phys. Rept.* 3 (1972) 261.
- [4] P. Vogel and J.F. Beacom, *Phys. Rev. D* 60 (1999) 053003.
- [5] See e.g. the recent review V. Cirigliano, G. Colangelo, G. Isidori, G. Lopez-Castro, D. Pokanic and B. Sciascia, “*Status of  $V_{us}$  and  $V_{ud}$* ”, to appear in the proceedings of the first CKM workshop, CERN, february 13–16, 2002.
- [6] I.S. Towner, *Phys. Rev. C* 58 (1998) 1288; J.F. Beacom and S.J. Parke, *Phys. Rev. D* 64 (2001) 091302; A. Kurylov, M.J. Ramsey-Musolf and P. Vogel, *Phys. Rev. C* 65 (2002) 055501.
- [7] A. Kurylov, M.J. Ramsey-Musolf and P. Vogel, hep-ph/0211306.
- [8] G. Fiorentini, M. Moretti and F.L. Villante, *Phys. Lett. B* 413 (1997) 378 and *Nucl. Phys. Proc. Suppl.* 70 (1999) 364.
- [9] M. Liebendorfer, A. Mezzacappa, F.K. Thielemann, O.E. Messer, W.R. Hix and S.W. Bruenn, *Phys. Rev. D* 63, 103004 (2001); M.T. Keil, G.G. Raffelt and H.T. Janka, astro-ph/0208035; A. Burrows and T.A. Thompson, astro-ph/0211404; C.L. Fryer, D.E. Holz, S.A. Hughes and M.S. Warren, astro-ph/0211609.
- [10] O.G. Ryazhskaya, L.V. Volkova and G.T. Zatsepin, *Nucl. Phys. Proc. Suppl.* 110 (2002) 358; The Super-Kamiokande collaboration, hep-ex/0212067.
- [11] M. Aglietta, et al, *Astropart. Phys.* 1 (1992) 1; Y. Fukuda *et al.*, *Astrophys. J.* 435 (1994) 225; The LVD collaboration, *Astron. and Astrophys.* 366 (2001) 573, astro-ph/0011249; The Super-Kamiokande collaboration, *Astrophys. J.* 578 (2002) 317, astro-ph/0205304.
- [12] The LSND collaboration, hep-ex/0104049; The KARMEN collaboration, hep-ex/0203021; E.D. Church et al., hep-ex/0203023.
- [13] C. Bemporad, G. Gratta and P. Vogel, *Rev. Mod. Phys.* 74 (2002) 297.
- [14] C.J. Horowitz, *Phys. Rev. D* 65 (2002) 043001.
- [15] N. Paver and Riazuddin, *Phys. Lett. B* 260 (1991) 421; J.F. Donoghue and D. Wyler, *Phys. Lett. B* 241 (1990) 243; N. Kaiser, *Phys. Rev. C* 64 (2001) 028201.
- [16] The CHOOZ collaboration, hep-ex/0301017.
- [17] The KamLAND collaboration, hep-ex/0212021.
- [18] See e.g. the recent reviews G.G. Raffelt, *Nucl. Phys. Proc. Suppl.* 110 (2002) 254 (hep-ph/0201099); S. Choubey and K. Kar, hep-ph/0212326 and references therein.
- [19] M. Aglietta et al., *Nucl. Phys. Proc. Suppl.* 110 (2002) 410.
- [20] P. Mergell, U.G. Meissner, D. Drechsel, *Nucl. Phys. A*596 (1996) 367.
- [21] S. Capitani *et al.*, *Nucl. Phys. Proc. Suppl.* 73, 294 (1999); M. Gockeler, R. Horsley, D. Pleiter, P.E. Rakow and G. Schierholz, hep-ph/0108105.
- [22] For a recent review on the axial structure of the nucleon see V. Bernard, L. Elouadrhiri, U.G. Meissner, *J. Phys. G*28 (2002) R1, hep-ph/0107088.
- [23] S.K. Singh and E. Oset, *Nucl. Phys. A*542 (1992) 687. For a theoretical discussion see R.E. Marshak, Riazuddin, C.P. Ryan, “*Theory of weak interactions in particle physics*”, Wiley, 1969.
- [24] D.H. Wright et. al. *Phys. Rev. C*57 (1998) 373.
- [25] P. Kammel et al., nucl-ex/0202011.
- [26] The Super-Kamiokande collaboration, *Phys. Rev. Lett.* 90 (2003) 061101 (hep-ex/0209028) and references therein. We thank M.S. Malek for interesting communications.
- [27] T. Totani, K. Sato, Y. Yoshii, *Astrophys. J.* 460 (1996) 303; R.A. Malaney, *Astropart. Phys.* 7 (1997) 125; D.H. Hartmann, S.E. Woosley, *Astropart. Phys.* 7 (1997) 137; M. Kaplinghat, G. Steigman, T.P. Walker, *Phys. Rev. D* 62 (2000) 043001.
- [28] T.J. Loredo and D.Q. Lamb, *Phys. Rev. D* 65 (2002) 063002.
- [29] G. Battistoni, A. Ferrari, T. Montaruli and P.R. Sala, hep-ph/0207035, *Astropart. Phys.* in print.